BioArchitecture 2:6, 214–219; November/December 2012; © 2012 Landes Bioscience

Fibroblast Growth Factor Receptor 3 regulates microtubule formation and cell surface mechanical properties in the developing organ of Corti

Katherine B. Szarama,[1,2,3,*] Ruben Stepanyan,[4] Ronald S. Petralia,[5] Nuria Gavara,[1,†] Gregory I. Frolenkov,[4] Matthew W. Kelley[2] and Richard S. Chadwick[1,*]

[1]Auditory Mechanics Section; Laboratory of Cellular Biology; National Institute on Deafness and Other Communication Disorders; National Institutes of Health; Bethesda, MD USA; [2]Laboratory of Cochlear Development; National Institute on Deafness and Other Communication Disorders; National Institutes of Health; Porter Neuroscience Research Center; Bethesda, MD USA; [3]Department of Clinical Science; Intervention and Technology; Karolinska Institutet; Stockholm, Sweden; [4]Department of Physiology; University of Kentucky; Lexington, KY USA; [5]Advanced Imaging Core; National Institute on Deafness and Other Communication Disorders; National Institutes of Health; Bethesda, MD USA

[†]Current Affiliation: Drittes Physikalisches Institut; Georg-August-Universität; Göttingen, Germany

Keywords: hair cell, pillar cell, Young's modulus, Fibroblast growth factor

Abbreviations: OHC, outer hair cell; PC, pillar cell; IHC, inner hair cell; Fgf, Fibroblast growth factor; P, postnatal day; μM, micro-Molar; RNA, ribonucleic acid; cDNA, complementary deoxyribonucleic acid; PCR, polymerase chain reaction; CLIP, CAP-Glycine domain containing linker protein; s.e.m., standard error of the mean

Fibroblast growth factor (Fgf) signaling is involved in the exquisite cellular patterning of the developing cochlea, and is necessary for proper hearing function. Our previous data indicate that Fgf signaling disrupts actin, which impacts the surface stiffness of sensory outer hair cells (OHCs) and non-sensory supporting pillar cells (PCs) in the organ of Corti. Here, we used Atomic Force Microscopy (AFM) to measure the impact of loss of function of Fgf-receptor 3, on cytoskeletal formation and cell surface mechanical properties. We find a 50% decrease in both OHC and PC surface stiffness, and a substantial disruption in microtubule formation in PCs. Moreover, we find no change in OHC electromotility of Fgfr3-deficient mice. To further understand the regulation by Fgf-signaling on microtubule formation, we treated wild-type cochlear explants with Fgf-receptor agonist Fgf2, or antagonist SU5402, and find that both treatments lead to a significant reduction in β-Tubulin isotypes I and II. To identify downstream transcriptional targets of Fgf-signaling, we used QPCR arrays to probe 84 cytoskeletal regulators. Of the 5 genes significantly upregulated following treatment, *Clasp2*, *Mapre2* and *Mark2* impact microtubule formation. We conclude that microtubule formation is a major downstream effector of Fgf-receptor 3, and suggest this pathway impacts the formation of fluid spaces in the organ of Corti.

Introduction

Modulation of cytoskeletal dynamics through growth factor signaling pathways is one of the main effectors of tissue morphogenesis during organ development. The auditory sensory epithelium, located within the cochlea of the inner ear, is a particularly appealing structure to examine how growth factor signaling imparts both the maturation of the cytoskeleton and the static material properties of the cell. The architecture of this tissue has a characteristic patterning of one row of sensory inner hair cells and three rows of outer hair cells with several interdigitating non-sensory supporting cell subtypes. In the mouse, the organization of this sensory epithelium occurs during embryonic development,[1] but the rearrangements of cytoskeletal components of individual cells and the formation of fluid-filled extracellular spaces in the sensory epithelium occur during postnatal development.[2] One such fluid-filled space between the two rows of microtubule-dense PCs, the tunnel of Corti, has been predicted to permit a fluid traveling sound wave[3] that supports OHC amplification.[4] Furthermore, the presence of cellular material within this tunnel has been reported in cases of Alport Syndrome with sensorineural hearing loss,[5] suggesting a direct role for the tunnel of Corti in auditory function. Therefore, structural defects to extracellular spaces in the cochlea,[6-8] as well as supporting cell cytoskeletal defects, may have profound effects on auditory function.

One potential growth factor mediating the cellular architecture within the cochlea is the Fibroblast growth factor (Fgf) signaling pathway. The Fgf family of receptors regulates differentiation in

*Correspondence to: Katherine B. Szarama and Richard S. Chadwick; szaramak@nidcd.nih.gov and chadwick@helix.nih.gov
Submitted: 09/04/12; Revised: 09/20/12; Accepted: 09/21/12
http://dx.doi.org/10.4161/bioa.22332

both OHCs[9] and PCs.[10] Initial evaluations of cell stiffness indicate that Fgf-signaling also regulates cell surface mechanical properties within the developing organ of Corti.[11] Finally, mutations that alter the dosage of Fgf-receptor 3 result in cochlear impairment and profound hearing loss in both mice and humans.[12,13] Here we test the hypothesis that the genetic ablation of Fgf receptor 3 (*Fgfr3*) reduces cytoskeletal components that contribute to the development of both cell mechanical properties and the formation of fluid-filled structures necessary for hearing function.

Fgfr3 Knockout Mice have Normal Outer Hair Cell Electromotility, but Disrupted Pillar Cell Morphology

We have previously shown that treatment with Fgf2, a strong ligand for all four Fgf-receptors, delays cell structural development and decreases stiffness at the OHC and PC surfaces in vitro.[11] To explore which Fgf receptor(s) could mediate the organization of the cytoskeleton and control the maturation of cell mechanical properties, we analyzed Fgfr3-deficient mice kindly provided by Dr. David Ornitz (Washington University in St. Louis, Missouri, USA). All genotypes were confirmed with PCR, which confirmed that the genetic deletion leads to a loss of both ligand binding and transmembrane domains of Fgfr3.[14] Mice were bred on a C57 black 6 background to generate *Fgfr3*$^{-/-}$ animals, which are viable but have a 60 dB hearing loss compared with wild-type littermates.[14] To determine whether defects in OHC function might underlie the hearing loss in these mutants, we first assessed the electromotility of OHCs, a phenomenon crucial for cochlear amplification.[15] We measured OHC voltage-dependent (nonlinear) capacitance, which results from translocation of the electrical charge across the plasma membrane during conformational changes of OHC membrane motors and is considered to be a "signature" of electromotility.[16] Organ of Corti explants were dissected at postnatal day 4 (P4) and cultured for 4 to 5 days in vitro before measuring outer hair cell capacitance with whole-cell patch-clamp recording techniques as described previously.[17] There was no statistically significant difference in nonlinear capacitance in OHCs of *Fgfr3*$^{-/-}$ and *Fgfr3*$^{+/-}$ mice (**Fig. 1A**). To compare between different cells, the capacitance was normalized to the cell surface area. No significant differences were observed in the maximal charge translocated across the plasma membrane, average linear (voltage-independent) capacitance, and the potential at the peak of nonlinear capacitance (**Fig. 1B**). We also noticed apparently normal mechano-electrical transduction in *Fgfr3*$^{-/-}$ OHCs (data not shown). Therefore, we conclude that Fgfr3 deficiency does not affect the normal development of the sensory and motor functions of OHCs.

Despite normal OHC electromotility, *Fgfr3*$^{-/-}$ mice have no detectable distortion product otoacoustic emissions,[7] which indicates that the loss of cochlear amplification is due to other factors. For example, defects to surrounding supporting cell structure may disrupt mechanical properties of the cochlear partition.[18] Therefore, we assessed how the loss of Fgfr3 impacts pillar cell structure. Cochleae from P3 mutants and heterozygous littermates were prepared for electron microscopy as previously

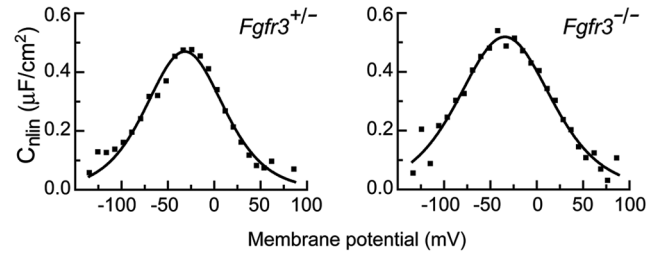

	z	Q_{max} (pC)	V_p (mV)	C_0 (pF)
Fgfr3$^{+/-}$	0.94±0.05	0.20±0.04	-31.1±1.64	6.5±0.39
Fgfr3$^{-/-}$	0.85±0.07	0.23±0.04	-36.1±10	6.4±0.24

Figure 1. Outer hair cell electromotility is normal in Fgfr3 knockout mice. (**A**) Voltage-dependent (nonlinear) component of OHC membrane capacitance in two representative cells approximately at the middle of the cochlea from control heterozygous (left) and Fgfr3 deficient (right) mice. Data were fit to the derivative of the Boltzmann function (solid line)

$$C_m(V) = C_0 + Q_{max}\frac{ze}{kT}\frac{b}{(1+b)^2}$$

where,

$$b = \exp\left(\frac{-2e(V-Vp)}{kT}\right)$$

C_0 is the voltage-independent (linear) capacitance, Q_{max} is the electrical charge transferred across the plasma membrane upon transition of the cell from fully extended to fully contracted state, V_p is the potential at the peak of $C_m(V)$, z is the effective valence of a charge moving from the inner to the outer aspect of the plasma membrane, k is Boltzmann's constant, T is absolute temperature (293 K), and e is the electron charge. (**B**) Boltzmann fit parameters (mean ± s.e.m.) in *Fgfr3*$^{-/-}$ (5 cells from 3 animals) and *Fgfr3*$^{+/-}$ (4 cells from 4 animals) OHCs. The errors of pClamp capacitance measurement algorithm were corrected offline as previously described[17] to account for a non-ideal ratio of the access resistance to the membrane resistance. To compare between OHCs, the voltage-dependent component of capacitance was divided by the surface area of the plasma membrane with the formula

$$X_m(V) = \frac{C_m(v) - C_0}{C_{0\acute{E}\ X_{lb}}}$$

where $X_m(V)$ is the specific nonlinear voltage-dependent capacitance of the plasma membrane in µF/cm² and X_{lb} = 1 µF/cm² is the specific capacitance of a lipid bilayer.

described.[11] Consistent with previous findings,[2,11] three types of supporting cells, the inner phalangeal cell, inner pillar cell, and outer pillar cell, were clearly present at the lumenal surface of the sensory epithelium between IHCs and the first row OHCs of *Fgfr3*$^{+/-}$ mice (**Fig. 2A**). Micrographs of Fgfr3 deficient mice showed a decrease in the supporting cell surface area between IHCs and OHCs relative to heterozygous littermates at P3 (**Fig. 2A**). In apical regions of Fgfr3 mutants, PCs protruding to the lumenal surface of the sensory epithelium were also smaller and lacked the characteristic bundles of microtubules (**Fig. 2B**) previously described in normally developing PCs.[11] To quantify this difference in tissue architecture, we calculated the average inner hair cell-to-outer hair cell (ITO) distance as previously

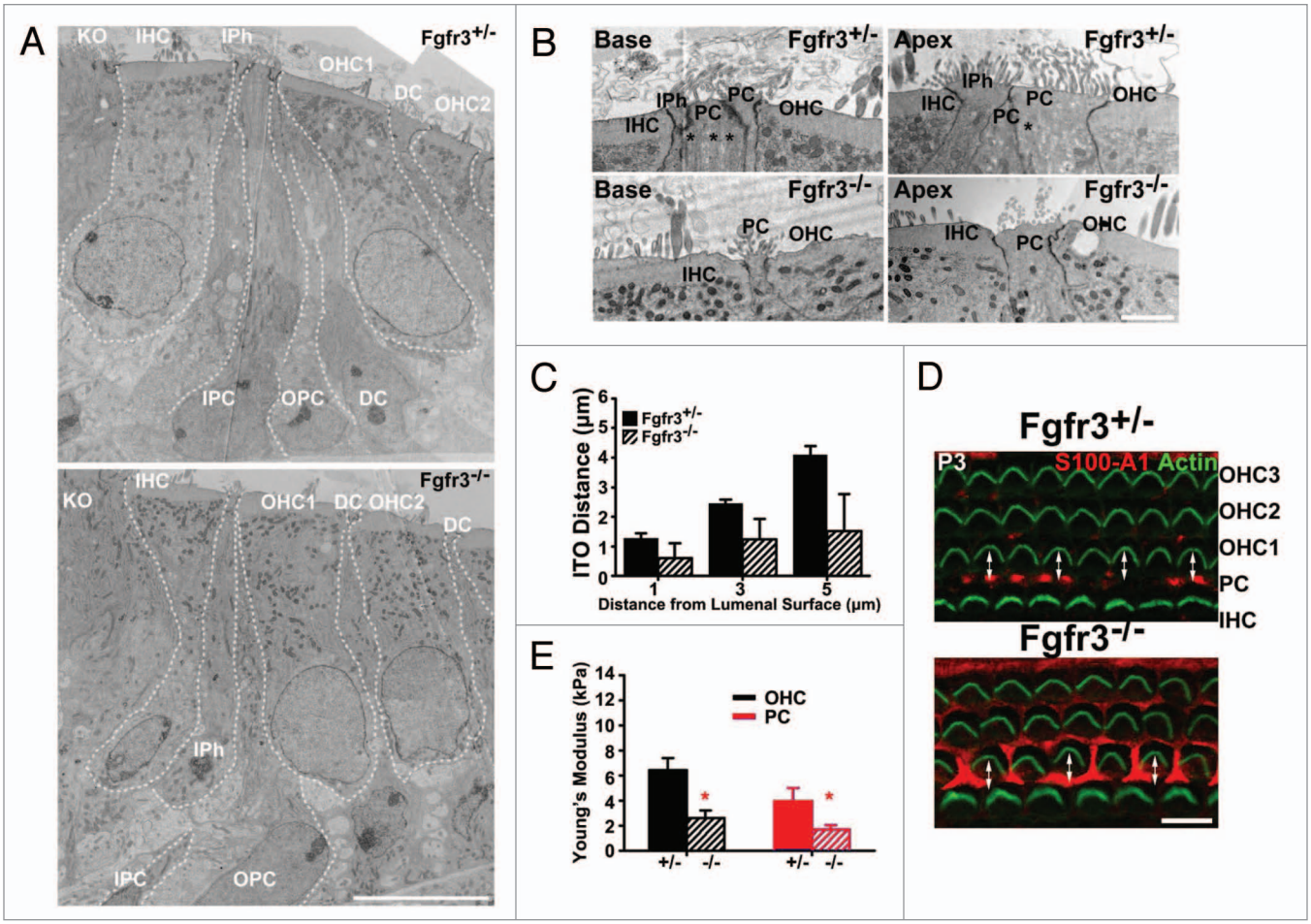

Figure 2. Fgfr3 knockout mice have underdeveloped pillar cells and decreased cell surface stiffness. (**A**) Representative electron micrographs of P3 cross-sections at the base of the cochlea show three supporting cells between IHCs and OHCs in *Fgfr3*$^{+/-}$ (top) and *Fgfr3*$^{-/-}$ (bottom). (**B**) Transmission electron micrographs of P3 cross-sections in the base and apex of the cochlea show microtubules (asterisks) in supporting cells between IHCs and OHCs lacking in *Fgfr3*$^{-/-}$ relative to *Fgfr3*$^{+/-}$ mice. (**C**) Average ITO distance (mean ± s.e.m.) measured from 4 micrographs each from 2 samples in mutant (hatched bars) compared with heterozygous (solid bars) mice. (**D**) Representative confocal z-projections of P3 basal cochleae labeled with an antibody against calcium binding protein S100-A1 expressed in supporting cells (red), and Phalloidin which stains filamentous actin (green), show the decreased distance between IHCs and OHCs in *Fgfr3*$^{-/-}$ relative to *Fgfr3*$^{+/-}$ mice. Double arrow lines represent 5 μm distance across the lumenal surface of the epithelium. (**E**) Average Young's modulus (mean ± s.e.m.) is significantly decreased when measured at the surface of both OHCs and PCs in *Fgfr3*$^{-/-}$ relative to *Fgfr3* $^{+/-}$ mice (*p-value < 0.05; student's t-test). Note that explants from 10–12 mice were examined for each condition. Scale bar, 10 μm, applies to (**A**). Scale bar, 2 μm, applies to (**B**). Scale bar, 10 μm, applies to (**D**). IHC, inner hair cell; OHC, outer hair cell; IPC, inner pillar cell; OPC, outer pillar cell; IPh, inner phalangeal cell, KO, Kölliker's organ; DC, Deiters' cell.

described[19] for 2 basal and 2 apical samples from 2 animals for each condition at 1 μm, 3 μm, and 5 μm distances from the lumenal surface of the pillar cell. Overall, a 50% decrease in the average ITO distance was observed at all three distances from the lumenal surface of the sensory epithelium (**Fig. 2C**). This difference could not be statistically tested with our small sample size. Therefore we also examined the lumenal surface of this epithelium by labeling P3 Fgfr3-mutant and heterozygous littermate supporting cells as previously described[11] with an antibody against calcium binding protein S100-A1 and phalloidin, which labels actin filaments. In these whole-mount preparations, we also observed a decreased distance between IHCs and the first row of OHCs in Fgfr3-deficient mice (**Fig. 2D**). These data indicate that while the same numbers of cells are present between the IHC and first row of OHCs in mutant and heterozygous cochleae, fewer cells protrude to the lumenal surface between the IHC and first row of OHCs in Fgfr3-deficient mice.

It is known that Fgf-signaling has direct implications on development of the actin cytoskeleton,[20] and that decreased Fgf-signaling can lead to patterning defects during cochlear development.[7,9,13,14] To examine the effects of Fgfr3-deficiency on cell surface mechanical properties, we measured the stiffness at different points across the surface of the sensory epithelium. Average Young's modulus for regions corresponding to OHCs and PCs was calculated as previously described[11] and compared between Fgfr3 knockout mice and heterozygous littermates. Results indicate that at P3, OHC Young's modulus (mean ± s.e.m) was decreased from 6.45 ± 0.95kPa to 2.59 ± 0.61kPa in *Fgfr3*$^{-/-}$ mice and PC Young's modulus was decreased from 3.95 ± 1.06kPa to 1.68 ± 0.38kPa in *Fgfr3*$^{-/-}$ mice relative to heterozygous

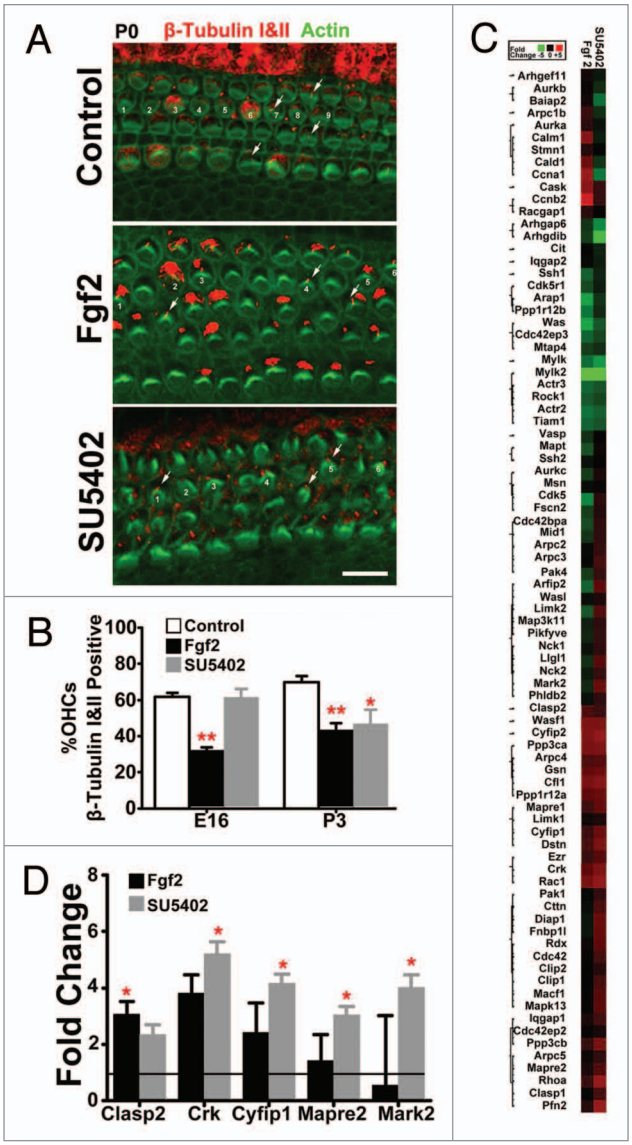

Figure 3. Both stimulation and antagonism of Fgf-signaling pathway disrupts microtubule formation in the developing cochlea. Cochlear explant cultures were treated with either SU5402 or Fgf2 and heparin sulfate for two days in vitro. (**A**) Confocal Z-projections of whole-mount preparations in apical regions of the cochlea labeled with anti- β-Tubulin I&II antibody (red) and direct-conjugated 488 Phalloidin (green) at postnatal day 0 (P0) show that β-Tubulin I&II localizes to OHCs (numbered 1–9). However cultures treated with Fgf2 or SU5402 show fewer β-Tubulin I&II positive OHCs (numbered 1–6). β-Tubulin I&II immunolabeled kinocilia are observed in all culture conditions (arrows). Scale Bar 20 μm. (**B**) Quantification of 100 OHCs repeated in apical regions of 5 samples for each condition shows that β-Tubulin I&II is significantly decreased in Fgf2-treated cultures (black bar) at embryonic day 16 (E16) and postnatal day 3 (P3), and in SU5402-treated cultures (gray bar) at P3 relative to controls (white bar) (data shown as mean ± s.e.m., *p-value < 0.05; **p-value < 0.01; student's t-test). (**C**) Clustergram displaying normalized fold increase/decrease (red/green) of 84 cytoskeletal regulators. Eighteen clusters of 2 or more genes were determined using hierarchical clustering in RT^2 Profiler^{TM} PCR array data analysis software (Qiagen). (**D**) Fold change gene expression of cytoskeletal regulators in Fgf2- and SU5402-treated conditions normalized to fold-change in control cultures. Significant differences are observed in fold change expression of Cytoplasmic linker-associated protein 2 (*Clasp2*) in Fgf2 treated cultures normalized to control conditions, while cytoplasmic tyrosine kinase adaptor molecule *Crk*, cytoplasmic Fragile X Mental Retardation-1 interacting protein 1 (*Cyfip1*), Microtubule-associated protein End-Binding family member 2 (*Mapre2*), and *Mark2*, an enzyme in the ELKL motif kinase family of small serine/threonine protein kinases are significantly differentially expressed in SU5402-treated cultures when normalized to control cochleae.

littermates (**Fig. 2E**). Together, these results suggest that Fgfr3 does regulate microtubule formation in PCs, and that microtubules may contribute a significant part of the developing Young's modulus at the cell surface.

Disruptions to Fgf-Signaling Decrease Microtubule Formation in the Developing Cochlea

Since *Fgfr3*$^{-/-}$ mice have fewer microtubules in PCs, we set out to determine whether acute modulation of Fgf signaling would also influence microtubule formation in wild type mice. Therefore, cochlear explant cultures were established at E16, P0, and P3, and maintained 18 h in vitro with one of the following: Fgf2 and heparin sulfate to bind and activate Fgf-receptors, SU5402 to inhibit Fgf-receptor tyrosine kinase activity,[21] or vehicle control as previously described.[11] To confirm the effectiveness of these treatments, an antibody against p75 neurotrophin receptor (p75ntr) was used to assess differentiation of PCs, which showed increased p75ntr expression and supporting cell de-differentiation induced by Fgf2 treatment, and decreased p75ntr expression under SU5402 treated conditions as previously described.[11,19] At postnatal day 0 (P0), β-Tubulin I&II localized to the lateral side of the OHC below the lumenal surface (**Fig. 3A**), and is consistent with previous expression profiling of β-Tubulin isotypes during development in vivo.[22,23] By comparison with control cultures, Fgf2- and SU5402-treated cultures showed decreased β-Tubulin I&II fluorescence (**Fig. 3A**). To quantify this difference, OHCs were counted as positive or negative for β-Tubulin I&II fluorescence (**Fig. 3A**), as untreated OHCs contained β-Tubulin I&II at all time-points measured. Then the percent of positively labeled OHCs per culture (mean ± s.e.m.) was calculated and compared between control and treated conditions. Cultures treated with Fgf2 had a significantly lower percentage of β-Tubulin I&II labeled cells at E16 and P3 when compared with control conditions, while SU5402-treated cultures showed a significant decrease in β-Tubulin I&II only at P3 (**Fig. 3B**). These data suggest that disruptions to Fgf-signaling lead to decreased levels of β-Tubulin in apical regions, which, over time, may contribute to the observed patterning disruption and auditory deficits in Fgfr3-deficient cochleae.

To identify potential downstream transcriptional targets of Fgf-dependent microtubule development in OHCs and PCs, cochleae were cultured and treated as previously described[11] for 2 days in vitro with one of the following: Fgf2, SU5402, or vehicle control. Six cochleae per condition were pooled for RNA extraction and cDNA synthesis using an RT^2 First Strand Kit (Qiagen). A gene expression panel of 84 cytoskeletal regulators was screened and repeated in triplicate for each condition using a

commercially available PCR array (PAMM-088ZA, Qiagen). To express similarity among relative gene expression levels, a hierarchical clustering method was used (RT^2 Profiler™ Software, Qiagen). This method applied the correlation coefficient as a similarity metric, as well as the absolute expression level and an average linkage method, to calculate the average distances between all pairs of genes. Based on this method, 18 clusters of genes were linked for these tissue samples (**Fig. 3C**), and one cluster of genes in particular (*Aurkc*, *Msn*, *Cdk5*, and *Fscn2*), which is involved in actin regulation and cell-cycle progression,[24,25] showed increased expression when treated with SU5402, and decreased expression when treated with Fgf2, relative to control conditions (**Fig. 3C**). Since no change in proliferation was observed in Fgfr3-deficient conditions[7,19] we examined the fold expression change normalized to a house-keeping gene panel of β2 microglobulin, glyceraldehyde 3-phosphate dehydrogenase, glucuronidase-β, and heat-shock protein-90, for each gene, and found significant differences between control and treated conditions in microtubule regulators (**Fig. 3D**). Cytoplasmic linker associated protein 2 (*Clasp2*) showed a significant 3-fold increase in expression in Fgf2 relative to control conditions (**Fig. 3D**). The protein product of this gene has been shown to stabilize a subset of microtubules[26] indirectly through binding with CLIPs and End-Binding (EB) proteins.[27,28] In SU5402-treated cochleae, statistically significant increases in expression of *Crk*, *Cyfip1*, *Mapre2*, and *Mark2* were observed relative to control cultures (**Fig. 3D**, p-value < 0.05). Cytoplasmic tyrosine kinase adaptor molecule, *Crk*, had a relative 5-fold higher expression in SU5402-treated cultures. Crk is a member of an adaptor protein family that binds to several tyrosine-phosphorylated proteins,[29,30] including Epidermal Growth Factor (EGF) receptor, upon stimulation with EGF.[31] These expression data suggest that a loss in Fgf-receptor tyrosine kinase activity may have a different regulatory cascade from stimulation of Fgf-receptors that can lead to upregulation of genes for adaptor molecules involved in receptor tyrosine kinase activities, as has been seen for mitogen-inducible genes.[20] Microtubule-associated protein RP/EB family member 2, *Mapre2*, had 3-fold higher gene expression in SU5402-treated relative to control conditions. *Mapre2* encodes the protein EB-2, which binds the plus-end of growing microtubules.[32] Enzyme in the ELKL Motif Kinase (EMK) family member Microtubule affinity regulating kinase 2, *Mark2*, had 4-fold higher gene expression in SU5402-treated relative to control conditions; it is a serine/threonine protein kinase involved in the control of cell polarity and is known to interact with doublecortin[33] and KIF13B.[34] The one exception to the characterization of cytoskeletal regulators involved in microtubule formation was *Cyfip1*, encoding a clathrin heavy chain binding protein that showed a 4-fold increase in gene expression and has been shown to interact with the product of the Fragile X Mental Retardation (FMR) gene.[35] FMR protein was first found to be responsible for Fragile X Syndrome, and it has been suggested that the phenotype observed in the central nervous system[36] is due to a disruption in protein synthesis, and, more recently, indirectly associated with remodeling of the actin cytoskeleton.[37] In summary, both stimulation and antagonism of the Fgf-signaling pathway alters the gene expression profile of different candidate microtubule regulators in the developing cochlea in vitro.

Conclusions

We have characterized the extent to which Fgfr3 contributes to developing microtubule structure and maturing cell surface mechanical properties. We show that while OHCs have normal electromotility in *Fgfr3* knockout mice, there is a lack of microtubule formation in PCs, indicating a disruption of the supporting cell patterning. Both PCs and Deiter's cells contain bundles of microtubules at postnatal stages, and disruptions to Fgfr3 lead to a decrease in microtubule formation. Therefore, it is reasonable to suggest that a lack of microtubules impairs the opening of extracellular spaces in this tissue. Indeed, we show that when microtubules are decreased, there is also a decrease in the distance between IHCs and the first row of OHCs. *Fgfr3* knockout mice also have a 50% reduction in surface stiffness of OHCs and PCs. However, microtubules are oriented to polymerize from the basolateral to the lumenal cell surface, and contribute only a part of the cell surface mechanical properties. Therefore, the Young's modulus may be different when measured from the lateral surfaces of these cells. Finally, we characterized the mechanism by which Fgf-signaling might regulate microtubule formation in the cochlea, and found 3 candidate cytoskeletal regulators previously shown to play a role in microtubule formation. However, because different gene expression profiles were significantly upregulated in Fgf2- and SU5402-treated conditions, we expect that this pathway may cross-talk with other signaling cascades in different cell types to affect microtubule formation. Taken together, our results suggest that the *Fgfr3*$^{-/-}$ mouse model featuring impaired microtubule development in supporting cells can lend further insight into the architecture necessary for proper hearing function.

Disclosure of Potential Conflicts of Interest

No potential conflicts of interest were disclosed.

Acknowledgments

We thank Ya-Xian Wang for help with tissue preparation for Electron Microscopy, and Drs. K. King and J. Bird for comments on this manuscript, and animal care staff involved. All animal care and procedures were approved by Animal Care and Use Committees and complied with NIH guidelines for the care and use of animals. This research was supported by the National Institute on Deafness and other Communication Disorders (NIDCD), Intramural Research Programs DC000059 to M.W.K., DC00003333 to R.S.C, R01 grant DC009434 to G.I.F., and in part with an Intramural Fellowship to Promote Diversity, from the NIH Office of the Director to K.B.S.

References

1. Lim DJ, Anniko M. Developmental morphology of the mouse inner ear. A scanning electron microscopic observation. Acta Otolaryngol Suppl 1985; 422:1-69; PMID:3877398
2. Souter M, Nevill G, Forge A. Postnatal maturation of the organ of Corti in gerbils: morphology and physiological responses. J Comp Neurol 1997; 386:635-51; PMID:9378857; http://dx.doi.org/10.1002/(SICI)1096-9861(19971006)386:4<635::AID-CNE9>3.0.CO;2-3
3. Karavitaki KD, Mountain DC. Evidence for outer hair cell driven oscillatory fluid flow in the tunnel of corti. Biophys J 2007; 92:3284-93; PMID:17277193; http://dx.doi.org/10.1529/biophysj.106.084087
4. Zagadou BF, Mountain DC. Analysis of the cochlear amplifier fluid pump hypothesis. J Assoc Res Otolaryngol 2012; 13:185-97; PMID:22302113; http://dx.doi.org/10.1007/s10162-011-0308-x
5. Merchant SN, Burgess BJ, Adams JC, Kashtan CE, Gregory MC, Santi PA, et al. Temporal bone histopathology in alport syndrome. Laryngoscope 2004; 114:1609-18; PMID:15475791; http://dx.doi.org/10.1097/00005537-200409000-00020
6. Gabrion J, Legrand C, Mercier B, Harricane MC, Uziel A. Microtubules in the cochlea of the hypothyroid developing rat. Hear Res 1984; 13:203-14; PMID:6376454; http://dx.doi.org/10.1016/0378-5955(84)90074-1
7. Puligilla C, Feng F, Ishikawa K, Bertuzzi S, Dabdoub A, Griffith AJ, et al. Disruption of fibroblast growth factor receptor 3 signaling results in defects in cellular differentiation, neuronal patterning, and hearing impairment. Dev Dyn 2007; 236:1905-17; PMID:17557302; http://dx.doi.org/10.1002/dvdy.21192
8. Inoshita A, Iizuka T, Okamura HO, Minekawa A, Kojima K, Furukawa M, et al. Postnatal development of the organ of Corti in dominant-negative Gjb2 transgenic mice. Neuroscience 2008; 156:1039-47; PMID:18793701; http://dx.doi.org/10.1016/j.neuroscience.2008.08.027
9. Pirvola U, Ylikoski J, Trokovic R, Hébert JM, McConnell SK, Partanen J. FGFR1 is required for the development of the auditory sensory epithelium. Neuron 2002; 35:671-80; PMID:12194867; http://dx.doi.org/10.1016/S0896-6273(02)00824-3
10. Mueller KL, Jacques BE, Kelley MW. Fibroblast growth factor signaling regulates pillar cell development in the organ of corti. J Neurosci 2002; 22:9368-77; PMID:12417662
11. Szarama KB, Gavara N, Petralia RS, Kelley MW, Chadwick RS. Cytoskeletal changes in actin and microtubules underlie the developing surface mechanical properties of sensory and supporting cells in the mouse cochlea. Development 2012; 139:2187-97; PMID:22573615; http://dx.doi.org/10.1242/dev.073734
12. Doherty ES, Lacbawan F, Hadley DW, Brewer C, Zalewski C, Kim HJ, et al. Muenke syndrome (FGFR3-related craniosynostosis): expansion of the phenotype and review of the literature. Am J Med Genet A 2007; 143A:3204-15; PMID:18000976; http://dx.doi.org/10.1002/ajmg.a.32078
13. Mansour SL, Twigg SR, Freeland RM, Wall SA, Li C, Wilkie AO. Hearing loss in a mouse model of Muenke syndrome. Hum Mol Genet 2009; 18:43-50; PMID:18818193; http://dx.doi.org/10.1093/hmg/ddn311
14. Colvin JS, Bohne BA, Harding GW, McEwen DG, Ornitz DM. Skeletal overgrowth and deafness in mice lacking fibroblast growth factor receptor 3. Nat Genet 1996; 12:390-7; PMID:8630492; http://dx.doi.org/10.1038/ng0496-390
15. Liberman MC, Gao J, He DZ, Wu X, Jia S, Zuo J. Prestin is required for electromotility of the outer hair cell and for the cochlear amplifier. Nature 2002; 419:300-4; PMID:12239568; http://dx.doi.org/10.1038/nature01059
16. Santos-Sacchi J. Reversible inhibition of voltage-dependent outer hair cell motility and capacitance. J Neurosci 1991; 11:3096-110; PMID:1941076
17. Frolenkov GI, Mammano F, Belyantseva IA, Coling D, Kachar B. Two distinct Ca(2+)-dependent signaling pathways regulate the motor output of cochlear outer hair cells. J Neurosci 2000; 20:5940-8; PMID:10934241
18. Minekawa A, Abe T, Inoshita A, Iizuka T, Kakehata S, Narui Y, et al. Cochlear outer hair cells in a dominant-negative connexin26 mutant mouse preserve non-linear capacitance in spite of impaired distortion product otoacoustic emission. Neuroscience 2009; 164:1312-9; PMID:19712724; http://dx.doi.org/10.1016/j.neuroscience.2009.08.043
19. Jacques BE, Montcouquiol ME, Layman EM, Lewandoski M, Kelley MW. Fgf8 induces pillar cell fate and regulates cellular patterning in the mammalian cochlea. Development 2007; 134:3021-9; PMID:17634195; http://dx.doi.org/10.1242/dev.02874
20. Chung HA, Hyodo-Miura J, Kitayama A, Terasaka C, Nagamune T, Ueno N. Screening of FGF target genes in Xenopus by microarray: temporal dissection of the signalling pathway using a chemical inhibitor. Genes Cells 2004; 9:749-61; PMID:15298682; http://dx.doi.org/10.1111/j.1356-9597.2004.00761.x
21. Mohammadi M, McMahon G, Sun L, Tang C, Hirth P, Yeh BK, et al. Structures of the tyrosine kinase domain of fibroblast growth factor receptor in complex with inhibitors. Science 1997; 276:955-60; PMID:9139660; http://dx.doi.org/10.1126/science.276.5314.955
22. Hallworth R, Ludueña RF. Differential expression of beta tubulin isotypes in the adult gerbil cochlea. Hear Res 2000; 148:161-72; PMID:10978833; http://dx.doi.org/10.1016/S0378-5955(00)00149-0
23. Jensen-Smith HC, Eley J, Steyger PS, Ludueña RF, Hallworth R. Cell type-specific reduction of beta tubulin isotypes synthesized in the developing gerbil organ of Corti. J Neurocytol 2003; 32:185-97; PMID:14707552; http://dx.doi.org/10.1023/B:NEUR.0000005602.18713.02
24. Cicero S, Herrup K. Cyclin-dependent kinase 5 is essential for neuronal cell cycle arrest and differentiation. J Neurosci 2005; 25:9658-68; PMID:16237170; http://dx.doi.org/10.1523/JNEUROSCI.1773-05.2005
25. Yokoyama T, Goto H, Izawa I, Mizutani H, Inagaki M. Aurora-B and Rho-kinase/ROCK, the two cleavage furrow kinases, independently regulate the progression of cytokinesis: possible existence of a novel cleavage furrow kinase phosphorylates ezrin/radixin/moesin (ERM). Genes Cells 2005; 10:127-37; PMID:15676024; http://dx.doi.org/10.1111/j.1365-2443.2005.00824.x
26. Akhmanova A, Hoogenraad CC, Drabek K, Stepanova T, Dortland B, Verkerk T, et al. Clasps are CLIP-115 and -170 associating proteins involved in the regional regulation of microtubule dynamics in motile fibroblasts. Cell 2001; 104:923-35; PMID:11290329; http://dx.doi.org/10.1016/S0092-8674(01)00288-4
27. Mimori-Kiyosue Y, Grigoriev I, Lansbergen G, Sasaki H, Matsui C, Severin F, et al. CLASP1 and CLASP2 bind to EB1 and regulate microtubule plus-end dynamics at the cell cortex. J Cell Biol 2005; 168:141-53; PMID:15631994; http://dx.doi.org/10.1083/jcb.200405094
28. Kumar P, Chimenti MS, Pemble H, Schönichen A, Thompson O, Jacobson MP, et al. Multisite phosphorylation disrupts arginine-glutamate salt bridge networks required for binding of cytoplasmic linker-associated protein 2 (CLASP2) to end-binding protein 1 (EB1). J Biol Chem 2012; 287:17050-64; PMID:22467876; http://dx.doi.org/10.1074/jbc.M111.316661
29. Matsuda M, Mayer BJ, Fukui Y, Hanafusa H. Binding of transforming protein, P47gag-crk, to a broad range of phosphotyrosine-containing proteins. Science 1990; 248:1537-9; PMID:1694307; http://dx.doi.org/10.1126/science.1694307
30. Matsuda M, Kurata T. Emerging components of the Crk oncogene product: the first identified adaptor protein. Cell Signal 1996; 8:335-40; PMID:8911681; http://dx.doi.org/10.1016/0898-6568(96)00067-8
31. Hashimoto Y, Katayama H, Kiyokawa E, Ota S, Kurata T, Gotoh N, et al. Phosphorylation of CrkII adaptor protein at tyrosine 221 by epidermal growth factor receptor. J Biol Chem 1998; 273:17186-91; PMID:9642287; http://dx.doi.org/10.1074/jbc.273.27.17186
32. Vitre B, Coquelle FM, Heichette C, Garnier C, Chrétien D, Arnal I. EB1 regulates microtubule dynamics and tubulin sheet closure in vitro. Nat Cell Biol 2008; 10:415-21; PMID:18364701; http://dx.doi.org/10.1038/ncb1703
33. Sapir T, Shmueli A, Levy T, Timm T, Elbaum M, Mandelkow EM, et al. Antagonistic effects of doublecortin and MARK2/Par-1 in the developing cerebral cortex. J Neurosci 2008; 28:13008-13; PMID:19036994; http://dx.doi.org/10.1523/JNEUROSCI.2363-08.2008
34. Yoshimura Y, Terabayashi T, Miki H. Par1b/MARK2 phosphorylates kinesin-like motor protein GAKIN/KIF13B to regulate axon formation. Mol Cell Biol 2010; 30:2206-19; PMID:20194617; http://dx.doi.org/10.1128/MCB.01181-09
35. Schenck A, Bardoni B, Moro A, Bagni C, Mandel JL. A highly conserved protein family interacting with the fragile X mental retardation protein (FMRP) and displaying selective interactions with FMRP-related proteins FXR1P and FXR2P. Proc Natl Acad Sci U S A 2001; 98:8844-9; PMID:11438699; http://dx.doi.org/10.1073/pnas.151231598
36. Schenck A, Bardoni B, Langmann C, Harden N, Mandel JL, Giangrande A. CYFIP/Sra-1 controls neuronal connectivity in Drosophila and links the Rac1 GTPase pathway to the fragile X protein. Neuron 2003; 38:887-98; PMID:12818175; http://dx.doi.org/10.1016/S0896-6273(03)00354-4
37. Anitei M, Stange C, Parshina I, Baust T, Schenck A, Raposo G, et al. Protein complexes containing CYFIP/Sra/PIR121 coordinate Arf1 and Rac1 signalling during clathrin-AP-1-coated carrier biogenesis at the TGN. Nat Cell Biol 2010; 12:330-40; PMID:20228810; http://dx.doi.org/10.1038/ncb2034